

PHOTOMETRY OF A GALACTIC FIELD AT $l = 232^\circ$, $b = -6^\circ$: THE OLD OPEN CLUSTER AUNER 1, THE NORMA-CYGNUS SPIRAL ARM, AND THE SIGNATURE OF THE WARPED GALACTIC THICK DISK

GIOVANNI CARRARO^{1,2}

Departamento de Astronomía, Universidad de Chile, Santiago, Chile; gcarraro@das.uchile.cl

ANDRÉ MOITINHO³

SIM/IDL, Faculdade de Ciências da Universidade de Lisboa, Lisbon, Portugal; andre@oal.ul.pt

MANUELA ZOCCALI

Department of Astronomy and Astrophysics, Universidad Católica de Chile, Santiago, Chile; mzoccali@astro.puc.cl

AND

RUBEN A. VÁZQUEZ AND GUSTAVO BAUME

Facultad de Ciencias Astronómicas y Geofísicas de la Universidad Nacional de La Plata, IALP-CONICET, La Plata, Argentina;

rvazquez@fcaglp.fcaglp.unlp.edu.ar, gbaume@fcaglp.fcaglp.unlp.edu.ar

Received 2006 April 28; accepted 2006 October 19

ABSTRACT

We perform a detailed photometric study of the stellar populations in a Galactic field at $l = 232^\circ$, $b = -6^\circ$ in the Canis Major (CMA) constellation. We present the first U , B , V , I photometry of the old open cluster Auner 1 and determine it to be ≈ 3.25 Gyr old and to lie 8.9 kpc from the Sun. In the background of the cluster, at more than 9 kpc, we detect a young population most likely associated with the Norma-Cygnus spiral arm. Furthermore, we detect the signature of an older population and identify its turnoff and red giant branch. This population is found to have a mean age of 7 Gyr and a mean metallicity of $Z = 0.006$. We reconstruct the geometry of the stellar distribution and argue that this older population, often associated with the CMA “galaxy,” in fact belongs to the warped old thin- and thick-disk components along this line of sight.

Key words: Galaxy: general — Hertzsprung-Russell diagram — open clusters and associations: general — open clusters and associations: individual (Auner 1)

Online material: color figures

1. INTRODUCTION

In recent papers (Carraro et al. 2005b; Moitinho et al. 2006; Vázquez et al. 2006) we have unveiled a new, detailed picture of the structure of the Milky Way’s disk in the third Galactic quadrant (3GQ). Our analysis of the young stellar population and molecular clouds that make up the Galactic thin disk has shown the following: (1) The Local arm, also called the Orion spur, apparently enters the 3GQ between $l = 220^\circ$ and 250° . It seems to remain close to the formal Galactic plane, $b = 0^\circ$, up to 5 kpc from the Sun, where it starts to descend abruptly, reaching $z = -1.5$ kpc below the plane at 9–11 kpc from the Sun. (2) The Local arm does not appear to be a grand design arm, but rather an interarm structure: a bridge emerging from the Carina-Sagittarius arm in the first quadrant and possibly reaching the Norma-Cygnus (outer) arm in the 3GQ. (3) The outer arm in the 3GQ is visible from $l = 200^\circ$ to 260° . We note that this picture bears some similarity to that sketched by Moffat et al. (1979) almost 30 years ago. (4) The presence of the Local and outer arms below the $b = 0^\circ$ plane is an effect of the warp of the Galactic disk (for further description of the warp, see May et al. [1997], Momany et al. [2006], Moitinho et al. [2006], and references therein). (5) The Perseus arm (mostly visible in the second quadrant) is not clearly traced in the 3GQ. (6) The young stellar and molecular warp reaches its southern

maximum at $l = 250^\circ$ – 260° . Evidence for the existence of an old population (4–10 Gyr) in the 3GQ has been reported by Bellazzini et al. (2004) and has been interpreted as a galaxy—the Canis Major (CMA) “galaxy”—undergoing an in-plane accretion onto the Milky Way. Besides the old population, the CMA galaxy has been thought to also contain a younger (1–2 Gyr) component, based on the presence of a blue sequence (commonly known as the “blue plume” [BP]) in color-magnitude diagrams (CMDs). But, as found by Carraro et al. (2005b) and confirmed in Moitinho et al. (2006) and Pandey et al. (2006), these blue stars are actually very young (≤ 100 Myr) and are seen in many different regions of the second quadrant and 3GQ. Notably, most of them were found to trace the Norma-Cygnus spiral arm in remarkable agreement with other tracers, such as CO molecular clouds and analytical models of spiral structure. As for a possible very old population associated with the CMA “galaxy,” which would be similar to those seen in almost all Local Group dwarf galaxies (Mateo 1998), Momany et al. (2006) have clearly shown that the lack of any extended blue horizontal-branch stars in its CMD argues against its existence in CMA. Thus, what seems to be left of the CMA “galaxy” is a *relatively metal-rich* ($-0.7 \leq [\text{Fe}/\text{H}] \leq 0.0$) intermediate-age (4–7 Gyr) population (Bellazzini et al. 2004). However, these age and metallicity ranges are suspiciously similar to those of the Galactic old thin or young thick disks (Norris 1999; Bensby et al. 2004).

In this paper we analyze a field in the constellation of CMA centered on the open cluster Auner 1. The observations reveal the signature of an intermediate-age, relatively metal-rich population

¹ Astronomy Department, Yale University, New Haven, CT, USA.

² ANDES Fellow, on leave from Dipartimento di Astronomia, Università di Padova, Padua, Italy.

³ CAAUL, Observatório Astronómico de Lisboa, Lisbon, Portugal.

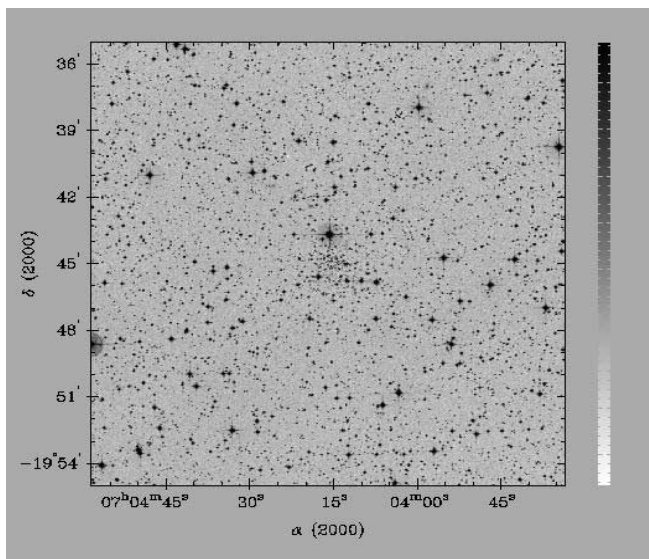


FIG. 1.—Blue Digital Sky Survey image of the area (20' on a side) discussed in this work. North is up, and east is to the left.

that, as we argue, belongs to the warped old thin or young thick disks.

2. OBSERVATIONAL MATERIAL

The U , B , V , I CCD photometry of the field under study was obtained at the Cerro Tololo Inter-American Observatory with the 1.0 m telescope operated by the SMARTS consortium.⁴ The telescope hosts a new $4K \times 4K$ CCD camera with a pixel scale of $0.289'' \text{ pixel}^{-1}$, which allows it to cover a field of $20' \times 20'$ on the sky. The field was observed on 2005 November 30, together with the Landolt (1992) fields T Phoenix, Rubin 149, PG 0231+006, and SA 95, to calibrate instrumental magnitudes to the standard system. The night was photometric, with an average seeing of $1.1''$. The data were reduced using the IRAF⁵ packages CCDRED, DAOPHOT, and PHOTCAL following the point-spread function method (Stetson 1987). An image of the covered area is shown in Figure 1. A more detailed discussion of the data reduction and calibration will be presented in a forthcoming paper (Vázquez et al. 2006).

3. THE OLD OPEN CLUSTER AUNER 1

The star cluster Auner 1 (R.A. = $07^{\text{h}}04^{\text{m}}16^{\text{s}}$, decl. = $-19^{\circ}45'$ [J2000.0]) was first detected by Auner et al. (1980) during a survey of hitherto unknown objects of various natures. No CCD study has yet been performed to our knowledge. The cluster is rather compact and faint, as can be seen by inspecting Figure 1.

We estimated the cluster radius by performing star counts around the cluster center using our photometric catalog. We employed the B and I bands to monitor absorption effects, since there seems to be some differential reddening toward the cluster. Indeed, the reddening map of the region from Schlegel et al. (1998) shows the presence of significant nebulosity on the southeast corner of the field and indicates a mean reddening $E(B - V)_{\text{FIRB}} = 0.60 \pm 0.15$ for this line of sight. From Figure 2 one can see how the cluster clearly stands out up to $2.5'$, and then a halo is visible in the I - (but not in the B -) band profile up to $3.5'$ before reaching

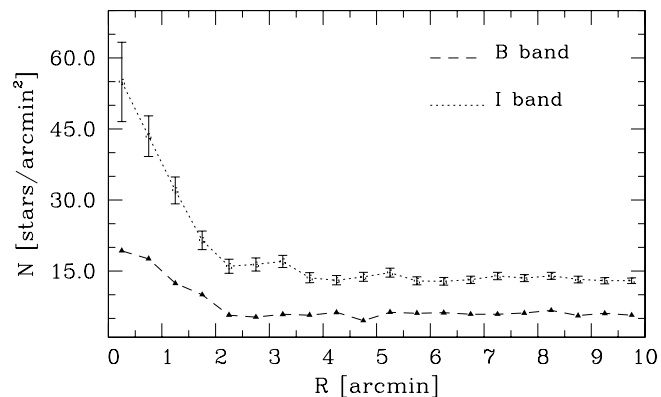


FIG. 2.—Radial density profile of the stars in the field of Auner 1. Star counts are made by using the B - and I -band magnitudes to emphasize absorption effects.

the level of the field. We therefore assign Auner 1 a radius of $3.0' \pm 0.5'$. This result is twice that listed in the open cluster catalog of Dias et al. (2002), which was based on visual inspection of the brightest stars.

The cluster’s fundamental parameters were derived by applying the isochrone fitting method using the Padova library of isochrones (Girardi et al. 2000), as illustrated in Figure 3. In the left panel we show the CMD of all the stars, whereas in the right panel we consider the results of the profile analysis and select only those stars within $3'$ of the cluster center. The cluster clearly emerges in this panel, whereas it is completely hidden in the left panel by the foreground and background population. The turnoff point (TO) is located at $V = 19.0$, $(V - I) = 0.9$; there is a readily detectable red giant branch (RGB) and a possible RGB clump of He-burning stars at $V = 16.8$. With a difference in magnitude between the TO and the red clump ΔV of 2.2 mag, Auner 1 would be 3.5 Gyr old (Carraro & Chiosi 1994).

We performed a detailed isochrone fitting analysis, and we show here the best fit, which is achieved for a 3.25 Gyr, $Z = 0.008 \pm 0.002$ isochrone, shifted by $E(B - V) = 0.32 \pm 0.05$ [$E(V - I) = 0.40 \pm 0.05$] and $(V - M_V) = 15.75 \pm 0.15$. This places the cluster at 8.9 kpc from the Sun. Accordingly, the Galactic Cartesian coordinates in the right-handed system in which the origin is placed at the Sun, the Galactic center is at $(0.0, -8.5, 0.0)$, and X increases toward $l = 90^\circ$ (Lynga 1982) are $X_G = -7.0$, $Y_G = 5.4$, and $Z_G = -0.9$ kpc, assuming $R_{GC,\odot} = 8.5$ kpc. The galactocentric distance is then 15.6 kpc.

Interestingly, this cluster falls in an age bin (3–4 Gyr; see Carraro et al. 2005a; Ortolani et al. 2005) in which only a few clusters were known before. Therefore, Auner 1 is a significant object for our understanding of the age distribution of the oldest open clusters.

4. THE STELLAR POPULATIONS IN THE FIELD OF AUNER 1

The presence of an almost vertical blue sequence in the V , $V - I$ CMD of Figure 3 (left), known as the “blue plume” (BP), which has already been detected in other clusters in this Galactic quadrant (Carraro et al. 2005b; Moitinho et al. 2006), and the location of Auner 1 at ~ 9 kpc from the Sun and ~ 1 kpc below the Galactic plane stress the complexity of the stellar populations in this region of the Galaxy. It is thus necessary to investigate in more detail the relation between Auner 1, the BP population, and the various Galactic disk components.

To provide a quantitative description of what is happening in this zone, we show in Figure 4 a series of two-color diagrams

⁴ See <http://www.astro.yale.edu/smarts/>.

⁵ IRAF is distributed by NOAO, which is operated by the Association of Universities for Research in Astronomy, Inc., under cooperative agreement with the NSF.

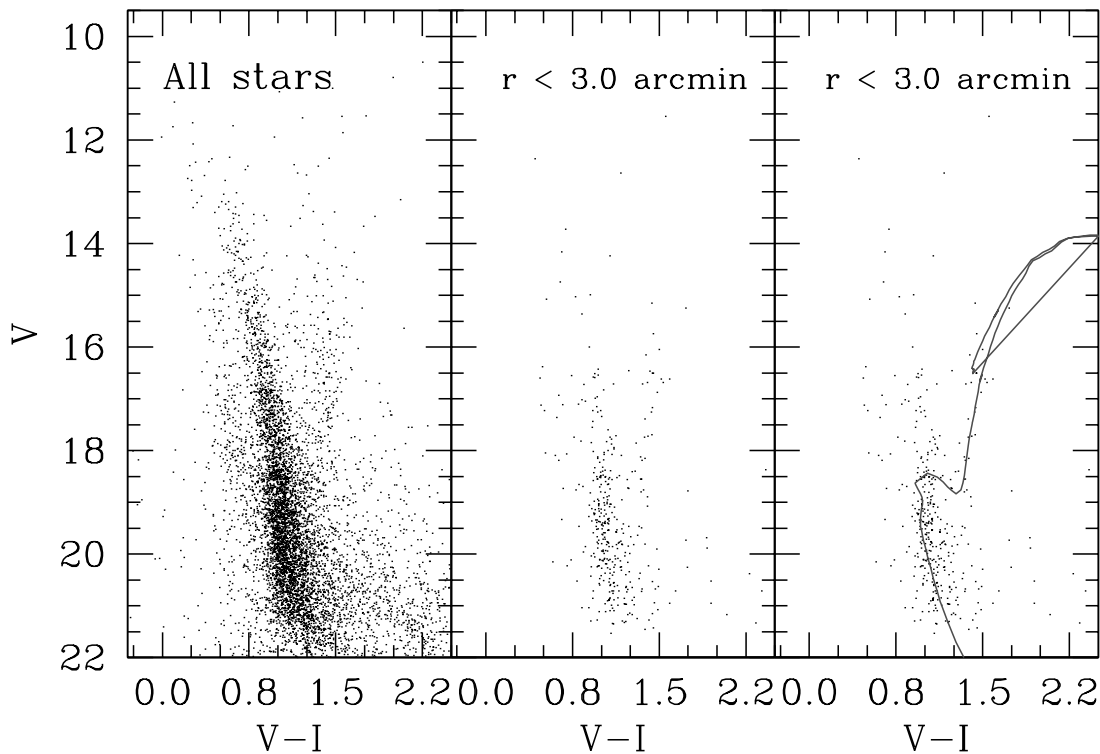


FIG. 3.—CMD of the whole field (*left*), the open cluster Auer 1 (*middle*), and the isochrone fitting (*right*). The $Z = 0.008$ isochrone has been shifted by $E(V - I) = 0.40$ and $(V - M)_V = 15.75$. All the stars are plotted without constraint on the photometric errors. [See the electronic edition of the *Journal* for a color version of this figure.]

(TCDs) including all the stars having $U - B$, $B - V$, and V in the entire observed field. Each TCD corresponds to a different magnitude bin in the CMD. The top middle panel is the TCD of the same stars plotted in the CMD. The top right panel is a reference diagram in which the solid line represents the intrinsic locus of unreddened dwarf stars (Schmidt-Kaler 1982); the positions of some spectral types and their absolute magnitudes are also indicated. The arrow indicates the way a star moves in this diagram when some reddening $E(B - V)$ takes place. The visual absorption is given by the standard relation $A_V = 3.1E(B - V)$, which was already found to hold in this region of the Galaxy (Moitinho 2001). The dashed line represents the locus occupied by giant stars of similar spectral types. In the analysis, special attention must be paid to the overlap region of dwarf, giant, and subgiant stars at $0.6 < B - V < 1.1$.

It is worth mentioning that all the stars plotted in Figure 4 have photometric errors < 0.10 mag in all the filters, a restrictive condition applied to minimize distortions in the diagrams. The solid diagonal line in the TCDs indicates the reddening path.

We point out that the procedure we are applying has been adapted from one developed long ago (see Fenkart et al. 1987) and is based on estimating the average reddening and distance of selected groups of stars according to the mean absolute magnitude of each group. An evident advantage of studying the stellar populations in magnitude bins is the simplicity of the morphology of the respective TCDs in contrast to the complex appearance of the global TCD (Fig. 4, *top middle panel*).

4.1. Results of the Method

The results of the whole procedure are summarized in Tables 1–4. Spectral types are assigned to the stars according to their position in the TCD. Mean distances and the number of stars in each spectral range are also reported. In these tables N is the number of stars and d is the heliocentric distance in kiloparsecs.

Figure 5 provides a graphical representation of the tables to facilitate their interpretation. This figure shows the trend of star counts with heliocentric distance for each spectral type range considered in the tables. Star count error bars have been plotted assuming a Poisson noise distribution. Star counts are not volume-normalized, the sole aim of the figure being to help the reader understand the various entries in the tables and the occurrence of different spectral type concentrations along the line of sight.

In Figure 5a we show the behavior of dwarf stars of spectral types from B6 to F0; in panel *b* we show the dwarf stars of spectral types from F0 to K0, together with the probable K0–K5 subgiants (SG) and dwarfs (D). In panel *c* we plot the same stars as in panel *b* but consider all the SG and D stars as dwarfs in deriving their distances and numbers. For this reason they are indicated with an asterisk. This is done in order to understand the effects and consequences of possible spectral type misinterpretations. Finally, in panel *d* the giant stars of all spectral types are shown.

The synoptic view of Figure 5 and Tables 1–4 allows us to derive the following:

1. Most of the stars with spectral types earlier than F0 are in the thin disk. This is an ensemble of early-type stars located at different distances along the line of sight. According to star counts, the BP stars (earlier than A5) are not evenly distributed along the line of sight, but they show some concentrations at 5, 9.5, and 12 kpc. Beyond 12–13 kpc the uncertainties in spectral type and distance derivation do not allow us to unambiguously detect any structure. These concentrations are compatible with the presence of the Local arm (5 kpc clump) and the Norma-Cygnus arm (9.5 and 12 kpc clumps) in this particular Galactic direction. The occurrence of such concentrations is typical of spiral arms, whose structure is irregular and clumpy.

2. An interesting point has been raised by the referee: whether the BP stars could, in fact, be halo A-type subdwarfs (sDA's). There are several reasons that indicate this is not the case. According

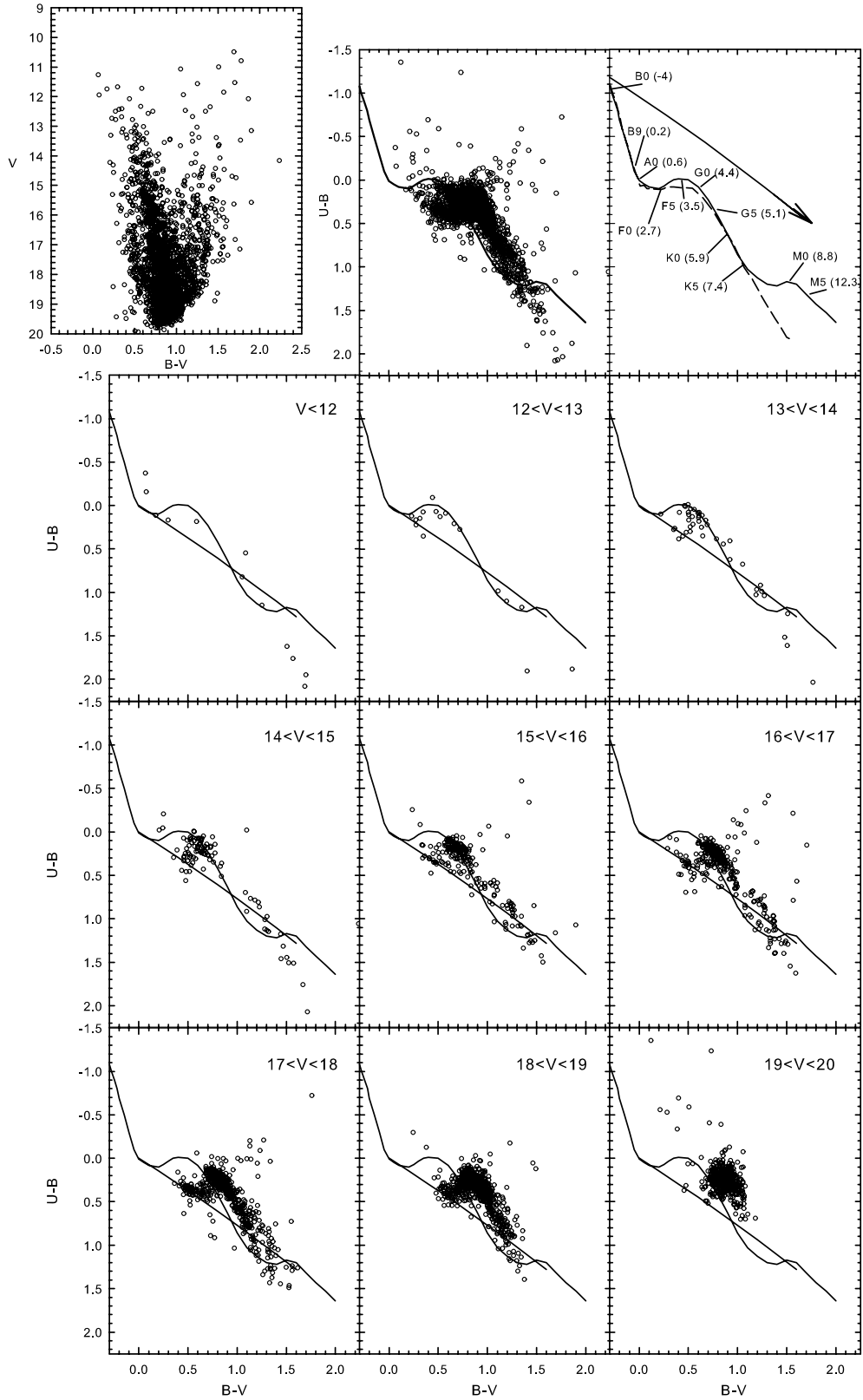


FIG. 4.— Detailed analysis of the population in the field of the open cluster Auner 1. Together with the cluster CMD, TCDs are shown at varying V magnitudes. Only stars with photometric errors lower than 0.1 in all the filters are shown. See the text for details.

TABLE 1
STAR COUNTS, REDDENING, AND SPECTRAL TYPE FOR EARLY-TYPE DWARF STARS IN AUNER 1

SPECTRAL TYPE	$\langle M_V \rangle$	<12 (0.2)		12–13 (0.1)		13–14 (0.25)		14–15 (0.3)		15–16 (0.45)		16–17 (0.50)		17–18 (0.6)		18–19 (0.65?)		19–20 (...)		TOTAL
		<i>N</i>	<i>d</i>	<i>N</i>	<i>d</i>	<i>N</i>	<i>d</i>	<i>N</i>	<i>d</i>	<i>N</i>	<i>d</i>	<i>N</i>	<i>d</i>	<i>N</i>	<i>d</i>	<i>N</i>	<i>d</i>	<i>N</i>	<i>d</i>	
B6–A0.....	–0.20	2	1.5	1	3.8	3	5.4	6	7.2	4	9.0	5	14.4	5	?	2	?	28
A0–A5.....	0.8	1	0.9	1	1.9	2	2.4	3	3.5	17	4.6	21	5.7	45	9.1	45	12.0	19	?	154
A5–F0.....	2.1	5	1.0	6	1.3	14	1.9	4	2.5	14	3.1	15	5.0	58

NOTE.—Headings contain V magnitude range and reddening (in parentheses).

TABLE 2
STAR COUNTS, REDDENING, AND SPECTRAL TYPE FOR LATE-TYPE DWARF STARS IN AUNER 1

SPECTRAL TYPE	$\langle M_V \rangle$	<12 (0.0)		12–13 (0.0)		13–14 (0.0)		14–15 (0.0)		15–16 (0.0)		16–17 (0.1)		17–18 (0.2)		18–19 (0.3)		19–20 (0.3)		TOTAL
		<i>N</i>	<i>d</i>	<i>N</i>	<i>d</i>	<i>N</i>	<i>d</i>	<i>N</i>	<i>d</i>	<i>N</i>	<i>d</i>	<i>N</i>	<i>d</i>	<i>N</i>	<i>d</i>	<i>N</i>	<i>d</i>	<i>N</i>	<i>d</i>	
F0–G0.....	3.4	1	0.4	5	0.6	12	1.0	19	1.6	10	2.6	36	3.6	125	5.0	219	6.8	216	10.4	643
G0–K0.....	4.9	1	0.2	1	0.3	11	0.5	31	0.8	87	1.3	91	1.7	152	5.2	374
K0–K5.....	6.5	2	0.2	2

NOTE.—Headings contain V magnitude range and reddening (in parentheses).

TABLE 3
STAR COUNTS, REDDENING, AND SPECTRAL TYPE FOR LATE-TYPE DWARF STARS OR SUBGIANT STAR CANDIDATES IN AUNER 1

SPECTRAL TYPE	$\langle M_V \rangle$	<12 (0.0)		12–13 (0.0)		13–14 (0.0)		14–15 (0.0)		15–16 (0.0)		16–17 (0.1)		17–18 (0.2)		18–19 (0.3)		19–20 (...)		TOTAL
		<i>N</i>	<i>d</i>	<i>N</i>	<i>d</i>	<i>N</i>	<i>d</i>	<i>N</i>	<i>d</i>	<i>N</i>	<i>d</i>	<i>N</i>	<i>d</i>	<i>N</i>	<i>d</i>	<i>N</i>	<i>d</i>	<i>N</i>	<i>d</i>	
G0–K0.....	3.9	181	4.0	278	5.2	459
K0–K5.....	1.7	5	2.3	7	3.6	42	5.7	48	7.9	89	11.0	91	14.0	282

NOTE.—Headings contain V magnitude range and reddening (in parentheses).

TABLE 4
STAR COUNTS, REDDENING, AND SPECTRAL TYPE FOR GIANT STARS IN AUNER 1

SPECTRAL TYPE	$\langle M_V \rangle$	<12 (0.2)		12–13 (0.1)		13–14 (0.15)		14–15 (0.2)		15–16 (0.25)		16–17 (0.25)		17–18 (0.3)		18–19 (...)		19–20 (...)		TOTAL
		<i>N</i>	<i>d</i>	<i>N</i>	<i>d</i>	<i>N</i>	<i>d</i>	<i>N</i>	<i>d</i>	<i>N</i>	<i>d</i>	<i>N</i>	<i>d</i>	<i>N</i>	<i>d</i>	<i>N</i>	<i>d</i>	<i>N</i>	<i>d</i>	
G0–K0.....	0.8	2	0.2	2
K0–K5.....	0.3	8	1.0	4	2.3	8	3.5	13	5.2	28	7.5	35	12.0	29	17.0	125
>K5.....	–0.5	1	3.4	2	5.0	2	7.5	1	10.9	6

NOTE.—Headings contain V magnitude range and reddening (in parentheses).

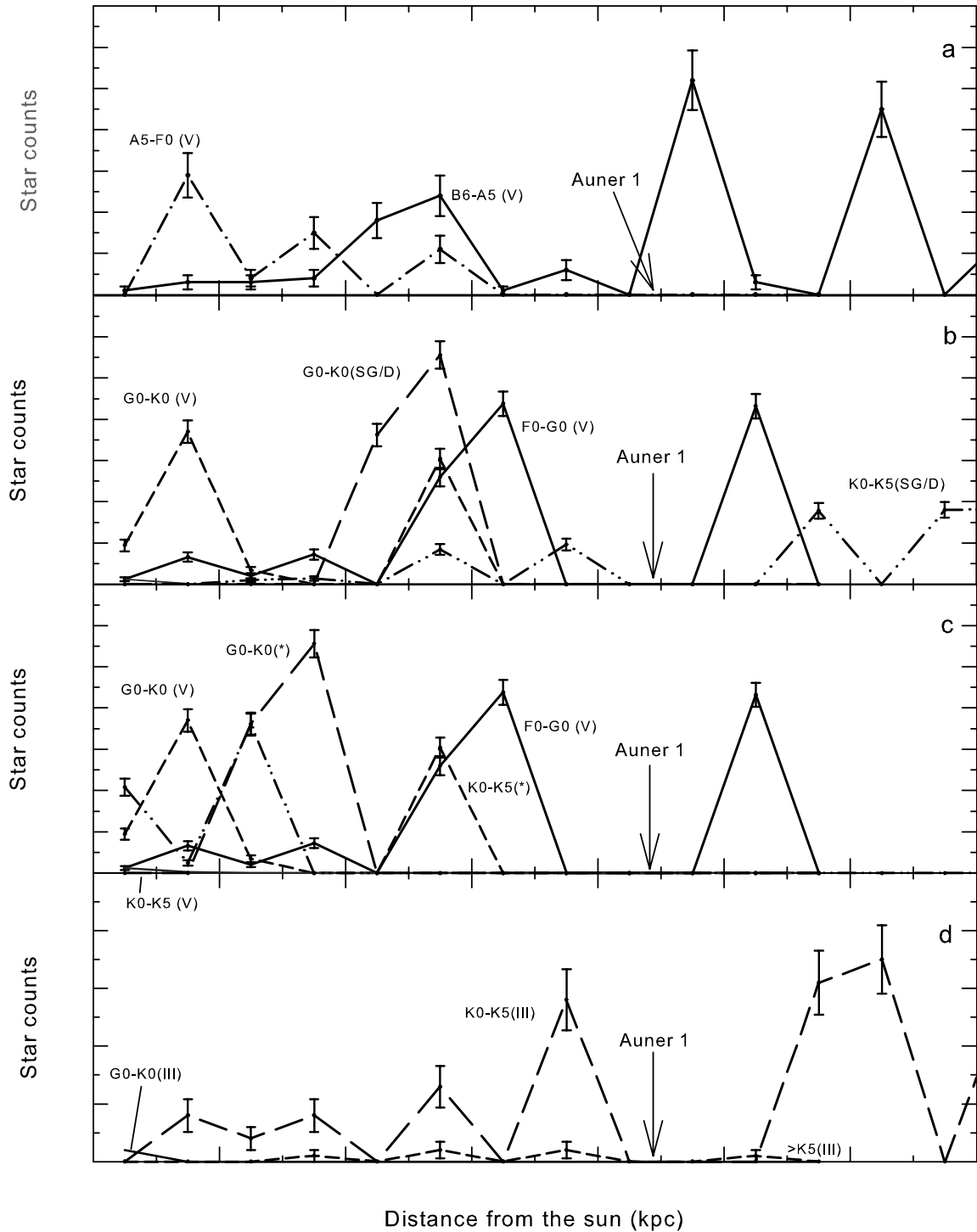


FIG. 5.—Trend of star counts as a function of heliocentric distance for stars of different spectral types in the direction of the old open cluster Auner 1.

to Thejll et al. (1997), with a mean $M_V \sim 4.5-5.0$ the sDA's would be located close to the Sun at less than 1.5 kpc. Also, the number of sDA stars would be $0.21 \text{ stars deg}^{-2}$ (Green et al. 1986), much less than the number of BP stars we find in our field. Furthermore, one would need to explain the clear lack of such a significant population of stars in the northern Galactic hemisphere, since the halo stars should also be seen there. The same kind of statistical considerations apply to the possibility that the BP stars might be blue stragglers. Finally, the BP in the field of Auner 1 is similar to those analyzed in our previous work (Carraro et al. 2005b; Moitinho et al. 2006), which

we have shown to be excellent spiral tracers. This latter result means that the BP must be young, independent of any photometric analysis.

3. The disk dwarfs (later than F0; Figs. 5b and 5c) show increasing concentration away from the Sun, with an interesting hole at about 8–10 kpc. This behavior is independent of a possible misclassification of dwarf and subgiant stars.

4. The thick-disk giants (Fig. 5d), although much less abundant, exhibit the same kind of distribution as the disk dwarfs.

5. The star cluster Auner 1, at a distance of ~ 9 kpc, lies where the distribution of thick-disk stars shows a minimum.

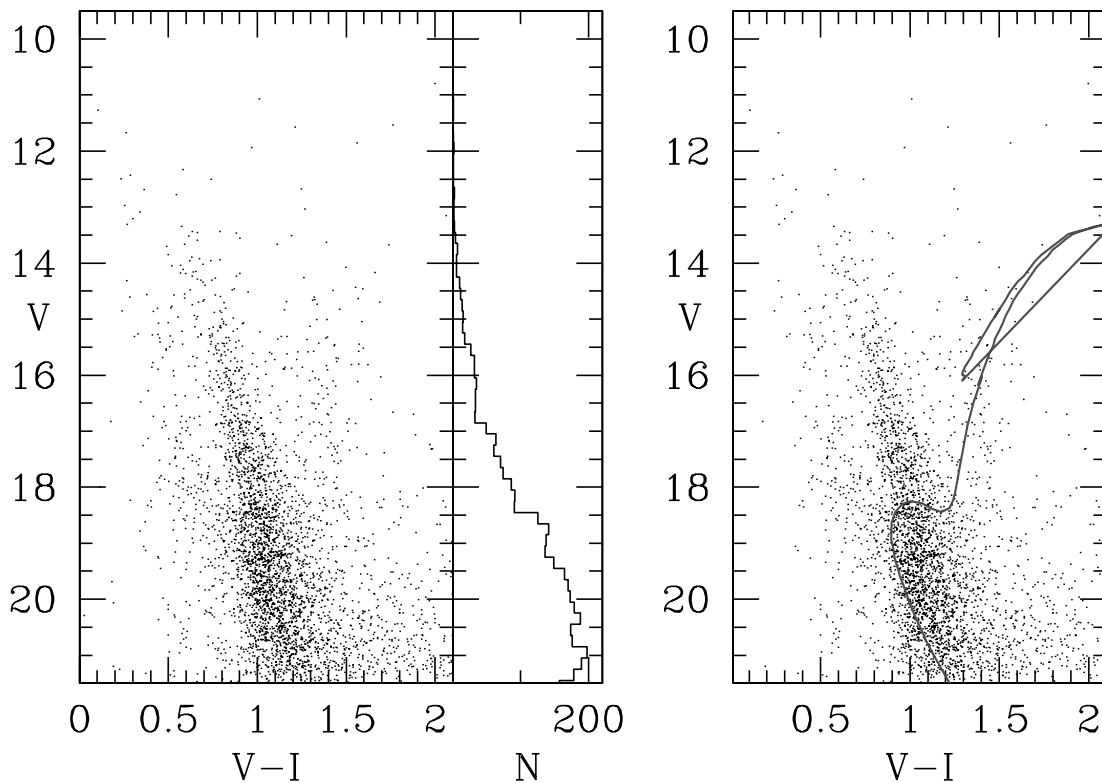


FIG. 6.—Old stellar population in the field of Auner 1. The left panel shows the CMD of all the stars outside the Auner 1 area, the middle panel shows the luminosity function of the main sequence, and the right panel presents a possible isochrone fitting to the old population. The $Z = 0.0067$ Gyr isochrone has been shifted by $E(V - I) = 0.35$ and $(V - M_V) = 15.5$. All the stars are plotted without constraint on the photometric errors. [See the electronic edition of the *Journal* for a color version of this figure.]

4.2. The BP, Auner 1, and Galactic Disk Components

The above analysis of the TCD series makes evident that the vertical blue sequence identified as the BP population is mostly composed of late B and early A-type stars from the group of stars found at 5.0 ± 1.5 kpc from the Sun. In brief, the BP stars compose a narrow band in the CMD and are young (≤ 100 Myr), with $0.30 < E(B - V) < 0.50$ and a distance modulus $15.7 < V - M_V < 16.3$. As the highest density of this type of star happens between 9 and 11 kpc from the Sun, we find this result entirely consistent with our previous results, in which we identified the BP stars as tracers of the Norma-Cygnus or outer arm (Carraro et al. 2005b; Moitinho et al. 2006; Baume et al. 2006). The other, nearer component (at 5 kpc, as stated above) probably belongs to the Local (Orion) arm. The nature of the BP stars has been clearly demonstrated in our diagrams, because most of the reddening happens in the first 6.5 kpc from the Sun (see Tables 1–4) and because the space behind must contain a small amount of dust. Therefore, the blue stars we see are simply far away and, for this reason, relatively faint.

Signatures of old thin- or thick-disk (subgiant, giant, and old dwarf stars) populations are also seen in the series of TCDs at the middle latitude of Auner 1, where we should expect to find a low density of them. Indeed, the TCDs show that red giant stars follow a pattern of increasing reddening (Fig. 4, moving from the $13 \leq V \leq 14$ panel to the $18 \leq V \leq 19$ panel); for this reason no obvious concentration, such as a red clump structure, appears. However, when looking toward Auner 1 we are also looking at the external border of the Galaxy, where the number of components of the thick disk, such as giant and subgiant stars, starts decreasing quickly.

For this reason, at $18 \leq V \leq 19$ the CMDs in Figures 3 and 4 show the lower envelope of the giant branch of the thick disk to be at $Z \simeq 1.0$ kpc below the Galactic plane (a reasonable limit for thick-disk components in a warped and flared structure). Below that magnitude range we continue to see very faint red dwarf stars, which also compose the thick disk.

It is worth emphasizing that this picture does not depend on the particular photometric error constraints we used. In fact, in Figures 3 and 6 we relaxed the error constraints when plotting all the point sources, showing that the scenario does not change.

5. DISCUSSION AND CONCLUSIONS

In a flat Galaxy, due to the location of the Sun within the crowded thin disk and to the low spatial density of the thick disk, we do not expect to detect clear signatures of the thick disk in a CMD for the following reasons: (1) Close to $b = 0^\circ$ there is high contamination from the thin disk. (2) Close to $b = \pm 90^\circ$ the number of disk (thin and thick) stars is small. (3) At intermediate longitudes there is less contamination from the thin disk, and an increased number of thick-disk stars are present, but the large spread in distances (and reddening) will not, in general, produce clear distinctive features in the CMD.

However, the situation is different when looking across a warped disk. Indeed, when facing the warp, the number of thick-disk stars is larger than when looking at $b = \pm 90^\circ$, and the number of thin-disk stars will be smaller than when looking along the disk ($b = 0^\circ$). At the same time, the thick-disk stars that follow the warp will be concentrated at approximately the same distance (when compared to the Sun-warp distance). These combined

effects will produce a recognizable sequence of thick-disk stars in a CMD (which will also include old thin-disk stars of similar age). Another expected effect is that, because the thick disk flares, it should still be detected at lower latitudes where the thin disk is no longer seen.

This is the case for the field we have analyzed in this paper, which includes the open cluster Auner 1. We have shown that the cluster is 3.25 Gyr old and lies 8.9 kpc from the Sun. In addition to the cluster population, we have detected other sequences, uniformly extended in our field, indicative of a young and an old field population. The occurrence of these young and old populations in the same field in the 3GQ is not confined to Auner 1. The XMM field discussed by Bellazzini et al. (2004, their Fig. 2) shows the same features, as well as a few open clusters, among them Tombaugh 1 (Carraro & Patat 1995), which is located at the same longitude and only 1° to the south of Auner 1.

Figure 3 shows that there is an excess of giant stars and a hump of blue stars around $V \sim 18.5$ and $(V - I) \sim 0.6$, which appears to be the TO of an evolved population. To emphasize this point, in Figure 6 we show the CMD of this region, which results from removing the open cluster Auner 1 (all the stars lying $7'$ from the cluster center without any error constraints). The TO of an older population, with its RGB and clump, remain and thus are not due to Auner 1. To make it clearer, in Figure 6 we also show a luminosity function (*middle panel*), which displays a weak but significant jump at $V \approx 18.5$ marking the TO of the old population.

Using isochrones to estimate the parameters of this population, we find that a $Z = 0.006 \pm 0.003$ ($[\text{Fe}/\text{H}] = -0.50$), 7 ± 1.0 Gyr isochrone (Fig. 6, *right*) provides a good description of the $V \sim 18.5$ TO region. This fit is achieved by shifting the isochrone by $E(B - V) = 0.35 \pm 0.10$ and $(V - M_V) = 15.5 \pm 0.5$, thus placing the bulk of this population at about 7.0 kpc from the Sun, consistent with the findings in Tables 1–4 and Figure 5.

Nevertheless, we emphasize that this fit is only indicative of the mean properties of this population. Indeed, the detailed analysis presented in Tables 1–4 clearly shows that the thick-disk population starts to be present at $V = 17.0$, reaching a maximum at ~ 18.5 . This indicates that the thick-disk stars are evenly distributed at all distances along this particular line of sight. Remarkably, this population possesses the typical features (age and metal content) of the old thin or young thick disk (Norris 1999; Bensby et al. 2004).

Further evidence for the Galactic nature of this population is given in Figure 7 by the CMDs of fields centered on the open cluster NGC 2414 (*first panel*; Moitinho 2001) and Haffner 9 (*second panel*; Vázquez et al. 2006) at $l \approx 232^\circ$ (almost the same l as Auner 1 and Tombaugh 1 but at $b = +1.94^\circ$ and -0.6° , respectively). These fields are well within the putative CMa “galaxy” (Bellazzini et al. 2004, their Fig. 1). However, they do not show the presence of the young BP or of the old TO (we call the attention of the reader to how the blue hump of stars, seen in the bottom two panels around $V \sim 18.5$, is not present in the top two panels). This suggests that, like the BP, the old population is not ubiquitous toward CMa (Carraro et al. 2005b) but seems to fol-

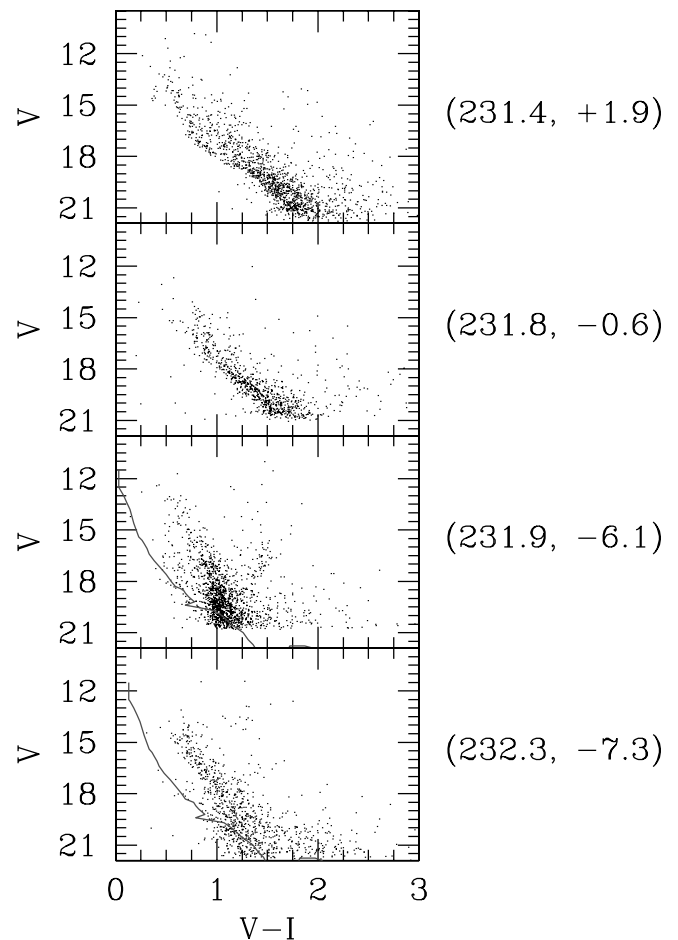


FIG. 7.—Stellar population in a vertical strip at $l \approx 232^\circ$. From the bottom to the top, the area-normalized CMDs of Tombaugh 1, Auner 1, Haffner 9, and NGC 2414 are shown. The solid line indicates the locus of the BP stars. [See the electronic edition of the *Journal* for a color version of this figure.]

low the pattern of the warped Galactic disk. In fact, the CMDs in Figure 7, normalized to the same area, show that in the case of Tombaugh 1 (*fourth panel*) the BP and old population are much less abundant than in Auner 1, reflecting the geometry of the Galactic disk and providing an estimate of the amplitude of the warp at this longitude. Moreover, a fit to the old background population in the field of Tombaugh 1 implies that it lies ≈ 9.0 kpc from the Sun, a few kiloparsecs more distant than the bulk of the old population in the field of Auner 1. Such an increase in distance is expected due to the warp, which would place increasingly distant stars at increasingly lower latitudes.

The authors deeply thank Jorge May for useful discussions. A. M. acknowledges support from FCT (Portugal) through grants SFRH/BPD/19105/2004 and PDCT/CTE-AST/57128/2004.

REFERENCES

- Auner, G., Dengel, J., Hartl, H., & Weinberger, R. 1980, *PASP*, 92, 422
 Baume, G., Moitinho, A., Vázquez, R. A., Solivella, G., Carraro, G., & Villanova, S. 2006, *MNRAS*, 367, 1441
 Bellazzini, M., Ibata, R. A., Monaco, L., Martin, N., Irwin, M. J., & Lewis, G. F. 2004, *MNRAS*, 354, 1263
 Bensby, T., Feltzing, S., & Lundström, I. 2004, *A&A*, 421, 969
 Carraro, G., & Chiosi, C. 1994, *A&A*, 287, 761
 Carraro, G., Geisler, D., Moitinho, A., Baume, G., & Vázquez, R. A. 2005a, *A&A*, 442, 917
 Carraro, G., & Patat, F. 1995, *MNRAS*, 276, 563
 Carraro, G., Vázquez, R. A., Moitinho, A., & Baume, G. 2005b, *ApJ*, 630, L153
 Dias, W. S., Alessi, B. S., Moitinho, A., & Lepine, J. R. D. 2002, *A&A*, 389, 871
 Fenkart, R., Topaktas, L., Boydag, S., & Kandemir, G. 1987, *A&AS*, 67, 245
 Girardi, L., Bressan, A., Bertelli, G., & Chiosi, C. 2000, *A&AS*, 141, 371
 Green, R. F., Schmidt, M., & Liebert, J. 1986, *ApJS*, 61, 305
 Landolt, A. U. 1992, *AJ*, 104, 340

- Lynga, G. 1982, *A&A*, 109, 213
Mateo, M. 1998, *ARA&A*, 36, 435
May, J., Alvarez, H., & Bronfman, L. 1997, *A&A*, 327, 325
Moffat, A. F. J., Jackson, P. D., & Fitzgerald, M. P. 1979, *A&AS*, 38, 197
Moitinho, A. 2001, *A&A*, 370, 436
Moitinho, A., Vázquez, R. A., Carraro, G., Baume, G., Giorgi, E. E., & Lyra, W. 2006, *MNRAS*, 368, L77
Momany, Y., Zaggia, S. R., Gilmore, G., Piotto, G., Carraro, G., Bedin, L., & de Angeli, F. 2006, *A&A*, 451, 515
Norris, J. E. 1999, *Ap&SS*, 265, 213
Ortolani, S., Bica, E., Barbuy, B., & Zoccali, M. 2005, *A&A*, 429, 607
Pandey, A. K., Sharma, S., & Ogura, K. 2006, *MNRAS*, 373, 255
Schlegel, D. J., Finkbeiner, D. P., & Davis, M. 1998, *ApJ*, 500, 525
Schmidt-Kaler, Th. 1982, in Landolt-Börnstein, Numerical Data and Functional Relationships in Science and Technology, New Series, Group VI, Vol. 2b, ed. K. Schaifers & H. H. Voigt (Berlin: Springer), 14
Stetson, P. B. 1987, *PASP*, 99, 191
Thejll, P., Flynn, C., Williamson, R., & Saffer, R. 1997, *A&A*, 317, 689
Vázquez, R. A., Carraro, G., May, J., Moitinho, A., Bronfmann, L., & Baume, G. 2006, *ApJ*, submitted